

A Study of the Interference from Sulphide and Dithionite on Electrochemical Sulphite Analyses on Platinum

Erling Skavås, Tor Hemmingsen*

University of Stavanger, 4036 Stavanger, Norway

*E-mail: tor.hemmingsen@uis.no

Received: 23 January 2007 / Accepted: 6 February 2007 / Published: 1 March 2007

The interference from sulphide and dithionite on the electrochemical analysis of sulphite on platinum in alkaline fresh water has been examined in the present study. Cyclic voltammetric experiments with a rotating disc electrode were used to examine how these compounds affect kinetics and the diffusion properties of sulphite. The reaction rate for the oxidation of sulphide was slow. Chronoamperometric experiments were therefore used to study this reaction. The results show that the linear relationship between the current density and the sulphite concentration that was found in a pure sulphite solution could not be obtained when sulphide and dithionite were also present in the solution.

Keywords: Sulphite; Dithionite; Sulphide; Interference; Cyclic voltammetry

1. INTRODUCTION

Sulphur compounds like sulphite and dithionite are sometimes used as oxygen scavengers to remove oxygen from closed water systems like e.g. district-heating systems. If an excess of sulphite or dithionite is added to the water, they may form reduced sulphur species such as sulphide, which will increase the corrosion rate of the pipelines. Control of the amount of sulphite and dithionite added to the water is therefore important in order to minimise the risk of an unpredicted high corrosion rate.

Several methods to determine the concentration of these compounds are described in the literature [1-5], but none of these methods is optimal for industrial use because the methods demanded periodic sampling and/or addition of analytical reagents often combined with time-consuming procedures [6].

Measurements by cyclic voltammetry have shown to be a useful technique to analyse sulphite in water at alkaline conditions [7]. However, sometimes a mixture of sulphur compounds is present as e.g. in the geothermic water used in district heating systems on Iceland [8]. In order to extend the method described above to solutions containing several sulphur compounds experiments were

performed to examine how sulphur compounds like dithionite and sulphide affect the current response from the sulphite oxidation.

Previous experiments in acidic solutions have shown that adsorbed sulphur influences the platinum electrode in aqueous solutions containing hydrogen sulphide [9].

2. EXPERIMENTAL

2.1. Methods

Cyclic voltammetric (CV) measurements were performed using a rotating disc electrode. The set-up is shown in Fig. 1. A three-electrode cell configuration was used consisting of a rotating platinum disc working electrode ($A = 0.20 \text{ cm}^2$), a stationary platinum counter electrode ($A = 0.48 \text{ cm}^2$) and a saturated calomel reference electrode. The electrodes were controlled using a bipotentiostat (Ecochemie), which was connected to a Hewlett Packard Pentium II PC with Windows 95 and PGSTAT 10 software. A modulated speed rotator from Pine Instrument Company rotated the working electrode. To obtain a fresh cross section surface of the working electrode it was polished for 5 minutes with SiC-emery paper, 4000 grit (Struers), and flushed with deionised water. If other values are not specified, a constant potential sweep rate of 20 mV/s was used in the CV experiments starting at a potential of -0.85 V versus a saturated calomel electrode (SCE, $+0.241 \text{ V}$ vs SHE).

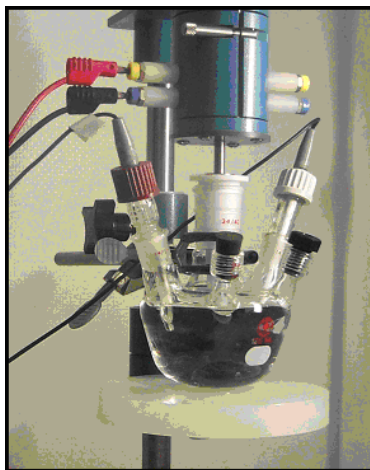


Figure 1. Cell configuration for the cyclic voltammetric experiments.

Chronoamperometry measurements were performed using a wall-jet flow cell. The set up of the wall-jet flow cell is based on the work of Gasana et al. [10] and is shown in Fig. 2. The cell has a three-electrode configuration with a high purity platinum disc working electrode, a graphite rod counter electrode and a saturated calomel reference electrode. An in-house fabricated working electrode was used. A platinum rod (3.0 cm length, 0.3 cm diameter) was positioned on a copper base to ensure electrical contact and covered with epoxy resin (Epofix kit, Struers) to give an exposed area of 0.071 cm^2 . A fresh electrode surface was obtained by polishing it with Buhler SiC-emery paper, type 1200, for 30 seconds. The surface was further polished on a Struers Planopol-2 polishing machine

using a polishing cloth with Buhler aluminium oxide powder of 1 and 0.05 μm particle size fineness for 5 and 10 minutes, respectively. The electrode was cleaned in an ultrasonic bath for 5 minutes in distilled water and for 5 minutes in ethanol.

The flow was directed onto the working electrode through a nozzle, positioned a few millimetres from the electrode. The flow rate was adjusted by a reduction valve and monitored on a flow meter. A peristaltic pump was used to circulate the electrolyte from the reservoir through the cell. The $[\text{Fe}(\text{CN})_6]^{4-}/[\text{Fe}(\text{CN})_6]^{3-}$ redox system was used to optimise the different parameters such as the flow rate and the distance between the nozzle and the electrode [10].

The potential was raised from the open circuit potential, E_{OCP} , where no reactions occur to a potential, E_2 , (in the potential region 0.95 – 1.20 V SCE) where a diffusion controlled oxidation reaction takes place.

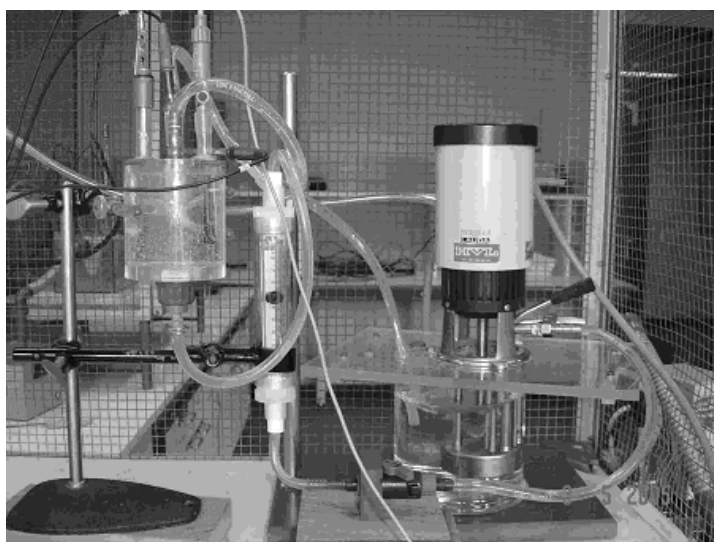


Figure 2. Wall-jet flow cell with pump unit.

2.2. Reagents

The water used in the experiment was purified through an ion exchange resin, and had a conductivity of 1.70 $\mu\text{S}/\text{cm}$. To obtain anaerobic conditions in the test electrolytes they were purged with nitrogen gas for at least 30 minutes prior to the addition of chemicals, and a nitrogen atmosphere was kept above the electrolyte as an inert layer during the electrochemical measurements.

0.5 M sodium hydroxide was used in order to obtain the appropriate pH values. The pH of the electrolyte was monitored through the experiment by the use of a pH electrode.

The chemicals used for making 1.0 M stock solutions were pro analysis qualities of sodium sulphite, sodium sulphide and sodium dithionite from Merck and sodium hydroxide from Riedel-de Haën. Fresh stock solution was stored in airtight containers equipped with septum. A syringe was used to transfer the solution from the container to the electrolyte.

Prior to each experiment deionised water was deaired by purging it with 99.999 % nitrogen gas for 30 minutes.

3. RESULTS AND DISCUSSION

The oxidation rate is controlled by kinetics of a reaction, diffusion rate of species to and from the electrode surface or a combination of these two processes depending on the applied potential. Cyclic voltammetry (CV) is best suited to identify these three distinct potential regions.

CV measurements were performed in alkaline electrolytes of dithionite, sulphite and sulphide in order to identify the oxidation potentials for each of these components using a platinum rotating disc electrode. The voltammograms for each of the sulphur compounds are shown in Fig. 3.

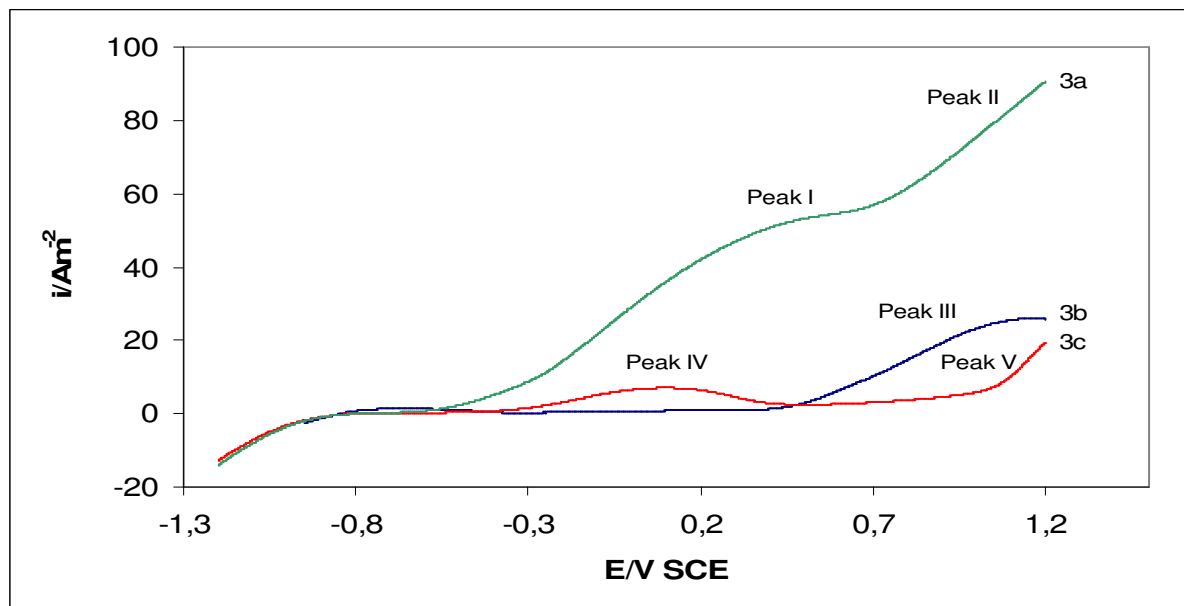


Figure 3. Voltammograms of 10 mM dithionite (3a), sulphite (3b) and sulphide (3c) in an alkaline fresh water solution. on a rotating disc electrode (1000 rpm). The sweep rate was 100 mV/sec, pH 11.

The voltammograms are labelled 3a for dithionite, 3b for sulphite and 3c for sulphide. An earlier study performed by Gasana et al [11] has shown that dithionite is oxidised in two distinct reaction steps with sulphite as a stable intermediate product. These current density peaks are also observed in Fig. 3. In the first reaction step dithionite is oxidised to sulphite. This reaction step starts at -0,55 V SCE, called peak I in Fig. 3, and leads to a current density plateau from 0,68 to 0,87 V SCE. The second reaction step, where the sulphite produced in the first reaction step is oxidised to a sulphite radical [12], starts at 0,87 V SCE. This peak is called peak II in Fig. 3. The current of peak II does not reach a plateau before the vertex potential at 1,2 V.

The voltammogram from the oxidation of sulphite has only one current peak, called peak III. It starts at 0,32 V SCE and reaches a plateau at 1,1 V SCE. The current plateaus for both sulphite and the first reaction step of dithionite (peak I) indicate that the reaction rate in this potential area is diffusion controlled.

For the sulphide solution a current density peak, called peak IV, is observed at approximately 0.1 V SCE. A second oxidation current density peak, called peak V, starts at approximately 0.85 V SCE. As for the second current peak in the voltammogram for oxidation of dithionite, the current of this peak does not reach a plateau before the vertex potential.

Sweep 3b and 3c in Fig. 3 show that the oxidation reaction of sulphite (peak II) and the second oxidation reaction step of sulphide (peak V) overlap in potentials. This will complicate the analysis of an unknown solution that contains sulphite and sulphide since it will be difficult to separate the current contribution from the oxidation of each of these compounds. Two separate CV experiments were performed to compare the linear sweep voltammogram from the oxidation of 10 mM sulphite solution with the voltammogram from the oxidation of a solution containing 10 mM sulphite and 5 mM sulphide. The results are shown in Fig. 4.

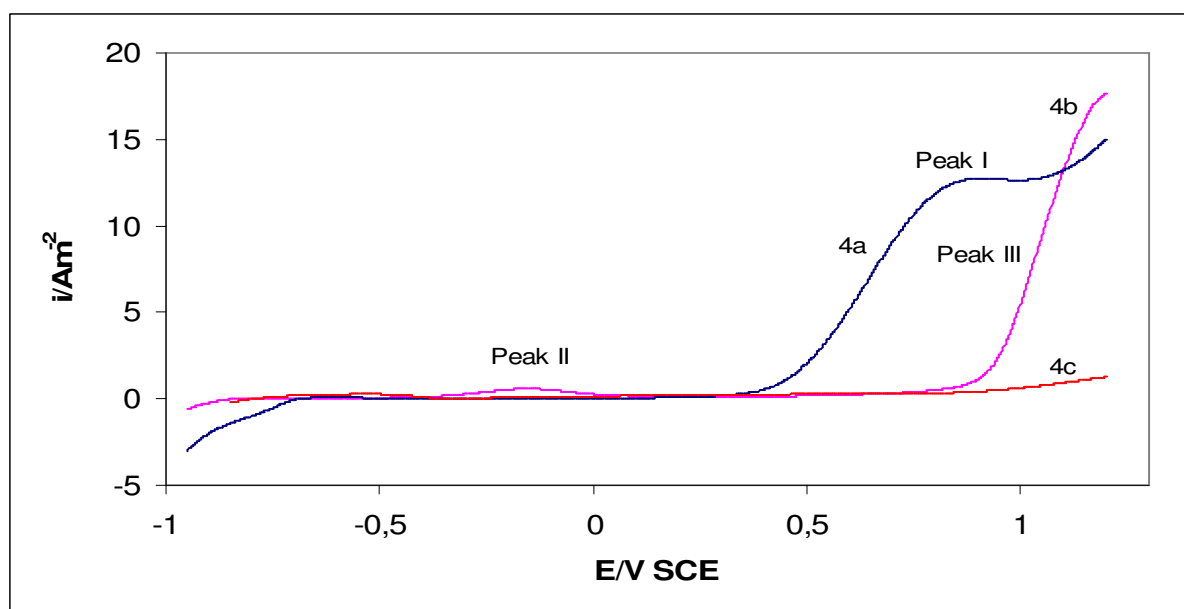


Figure 4. Linear sweep voltammogram of a 10 mM sulphite solution (4a), a 10 mM sulphite solution added 5 mM sulphide (4b) and water (4) at pH 11, sweep rate 20 mV/sec, rotation rate 1000 rpm.

As shown in Fig. 4, the presence of sulphide suppresses the oxidation current from sulphite. The current density peak from the oxidation of sulphite in sweep 4a, called peak I, disappears in sweep 4b. The current density peak, called peak III, starting at approximately 0.85 V SCE, probably arises from the oxidation of sulphide. A second current peak, called peak II, can be seen in the potential area from -0.35 to 0.1 V SCE in sweep 4b. This current density peak can also be seen in sweep 3c in Fig. 3 (peak IV), but in the mixed solution the peak potential is lowered and has a reduced peak current density.

Sweep 4a and 4b are obtained in separate experiments performed on a freshly polished platinum electrode. The product of the oxidation reaction that give rise to current peak II in Fig. 4 must therefore be involved in the disappearance of the sulphite oxidation peak since the second oxidation peak in sweep 4b occurs at a higher potential than the sulphite oxidation.

As can be seen from voltammogram 3c in Fig. 3 and 4b in Fig. 4 the kinetics of the first step in the oxidation reaction of sulphide is slow since the current density does not reach a limiting current plateau even at a relatively low potential sweep rate of 20 mV/sec. To investigate how the product of the sulphide reaction affects the behaviour of the platinum electrode at different potentials, CV experiments were performed in sequence, where the anodic vertex potential was increased in steps between each set of sweeps. The results are shown in Fig. 5.

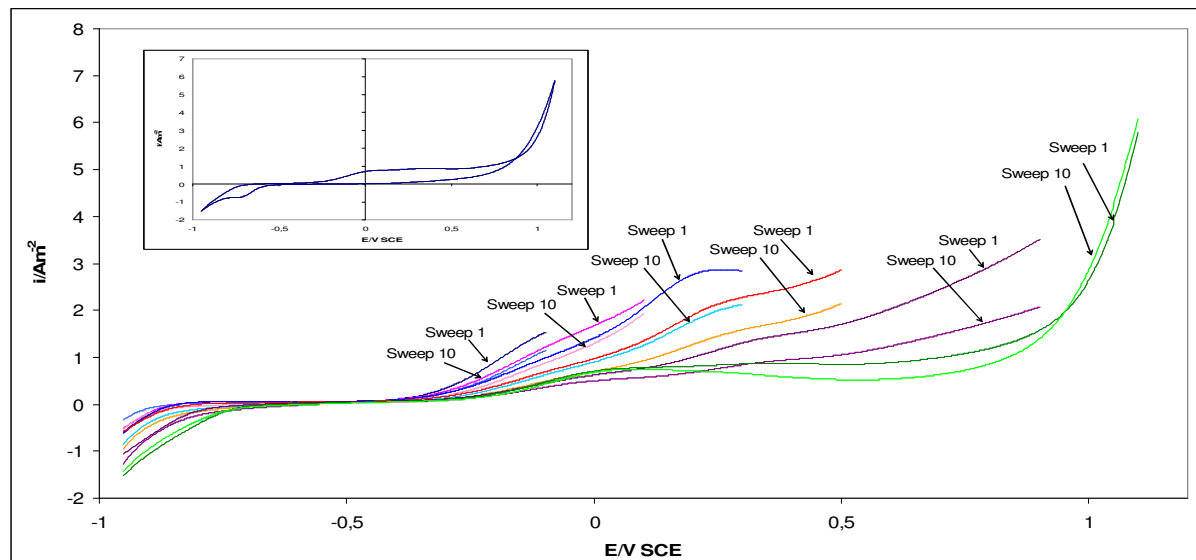


Figure 5. Voltammograms of 10 mM sodium sulphide solution (pH 11) on a RDE (1000 rpm) with a sweep rate of 20 mV/sec. The anodic vertex potential is varied from -0.1 to 1.1 V SCE.

The vertex potentials in Fig. 5 start at -0.1 V SCE and are increased in steps to 1.1 V SCE. Sweep 1 and sweep 10 are shown for each vertex potential. As can be seen from Fig. 5 the current density of the first oxidation step is decreasing from sweep 1 to sweep 10. For vertex potentials from -0.1 to 0.3 V SCE the current density of sweep 10 from one vertex potential is approximately equal to the current density of sweep 1 from the next vertex potential. The current density peak of the first oxidation step is reached between the vertex potential of 0.1 and 0.3 V SCE. As can be seen from Fig. 5, the current density peak of the first oxidation step decreases with increasing number of scans until it stabilises at approximately 0.75 A/m^2 .

Several sweeps are therefore needed to form a film that covers the electrode surface completely. This indicates that the kinetics of the film formation on the platinum electrode surface is very slow. Other studies have suggested that this film may be an oxide film with incorporated sulphide and that species such as Pt-S-O are formed on the surface [13].

The next oxidation step starts at a potential between 0.3 and 0.5 V SCE. The current density of this oxidation step is also decreasing with increasing numbers of sweeps. When the vertex potential was set to 1.1 V SCE, a sharp increase in the current density was observed at approximately 0.9 V SCE. The insert in Fig. 5 shows the whole cycle of sweep 1 when the vertex potential was set to 1.1 V SCE. It shows that the current density in the potential area from 0.9 to 1.1 V SCE is higher on the return sweep

than before the potential sweep direction is changed at 1.1 V SCE. This observation, where the anodic branches of the cyclic voltammogram cross twice, indicates that bulk overpotential deposition occurs via a nucleation process [14]. The reduction peak on the reverse sweep at approximately -0.7 V SCE was observed for all vertex potentials and is probably caused by the reduction platinum sulphide formed in the first oxidation step.

In order to examine if there is a correlation between the reduction of the current density and the increase in the vertex potential in Fig. 5, a new set of CV experiments were performed after the experiment with a vertex potential of 1.1 V SCE, where the vertex potential was decreased in steps between each set of sweeps. The results are shown in Fig. 6.

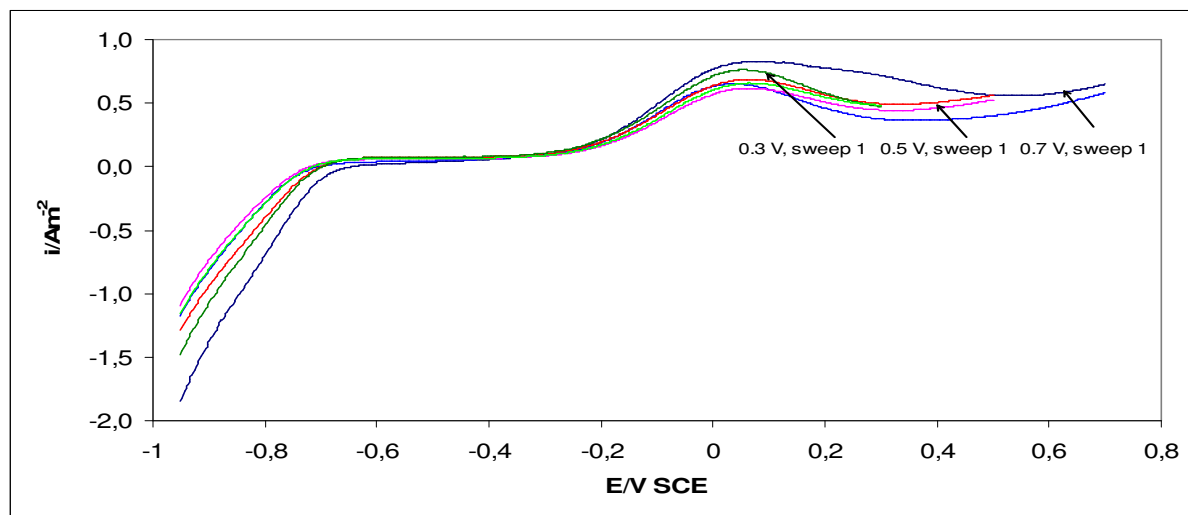


Figure 6. Cyclic voltammograms of an alkaline 10 mM sodium sulphide solution on a RDE (1000 rpm) with a sweep rate of 20 mV/sec. The anodic vertex potential is lowered from 0.7 to 0 V SCE. Sweeps 1 and 10 are shown for each vertex potential.

As can be seen from the data in Fig. 6, the current density peak of the first oxidation step is similar to what was obtained for the high vertex potentials in Fig. 5. The peak current density and the peak potential show a small variation between the different sweeps, most probably caused by change in the platinum sulphide film that influences the kinetics of the sulphide oxidation.

Visual observations of the platinum electrode after the CV experiments did not show a film on the surface. However, visual observations of the electrode after a chronoamperometric experiment, where the oxidation potential is maintained at much longer times than CV experiments, showed that the formation of a platinum sulphide film could be observed at longer exposure time, e.g. 60 minutes. Two sets of chronoamperometric experiments were performed. In the first experiment the potential was set to 0.55 V SCE. At this potential only the first step of the oxidation reaction occurs. Current curves as a function of time at different concentrations are shown in Fig. 7.

After the experiment the appearance of the electrode surface had changed from shiny to a flat finish. The electrode surface was examined using ESCA (Electron Spectroscopy for Chemical Analyses). The results showed that the film contained sulphur and platinum, but could not be used in

order to determine if polysulphide is formed. In a second experiment the potential was set at 1.2 V SCE, where both reaction steps in the sulphide oxidation reaction can take place. Current curves as a function of time are shown in Fig. 8.

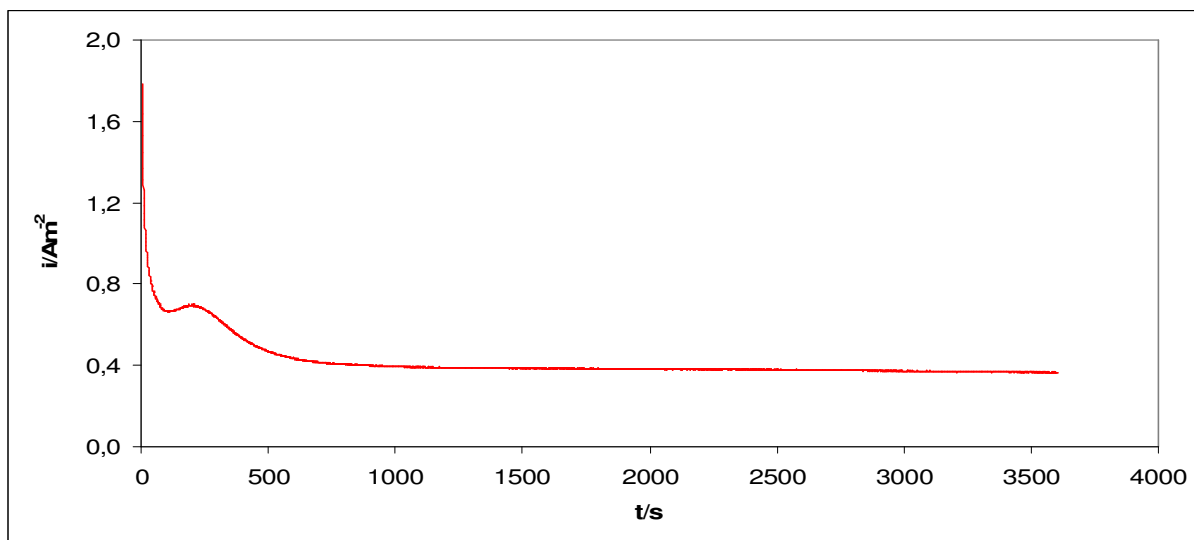


Figure 7. Chronoamperometry curves of the oxidation of sodium sulphide in the wall-jet flow cell at a potential of 0.55 V SCE. The flow rate is 1.2 litre/min, pH 11.

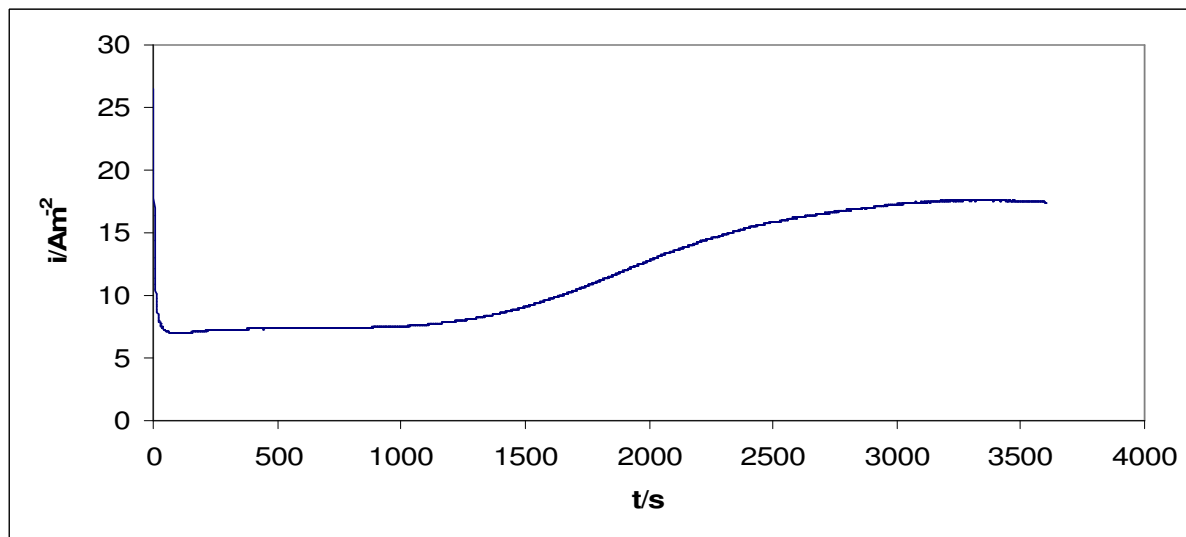


Figure 8. Chronoamperometry curve of the oxidation of sodium sulphide in the wall-jet flow cell at a potential of 1.20 V SCE. The flow rate is 1.2 litre/min, pH 11.

As shown in Fig. 8 the current density from the oxidation reaction is stable for approximately 1000 seconds before it starts to rise. After approximately the same amount of time a pale yellow film could be seen on the electrode surface. The surface film was analysed by Raman spectroscopy and found to

be elementary sulphur. Ultra low energy dynamic SIMS analysis [15] of the electrode surface under the layer of elementary sulphur showed presence of platinum sulphide.

The appearance of a maximum in the potentiostatic current transients, as seen in the experimental data, is usually associated with the existence of a nucleation and growth process [14,16]. This conclusion is supported by the CV findings, which showed the crossing phenomenon in the anodic branches [17]. The shape of the current transient in Fig. 7 indicates that the nucleation process is two-dimensional at 0.55 V SCE, while the shape of the current transient in Fig. 8 indicates that the nucleation process is three-dimensional at 1.2 V SCE [18].

Based on the experimental data with a sulphide solution the following sequence is proposed for the sulphide oxidation reaction. Starting at a potential of approximately -0.35 V SCE the platinum electrode is oxidised to platinum sulphide. The kinetics of this reaction step is very slow. In the next reaction step platinum sulphide is further oxidised to platinum disulphide. After some time the elementary sulphur is formed from the platinum polysulphide. The reaction sequence is shown schematically in Eq. 1.



The results reported by Kapusta et al [19] differ from our results. Kapusta reports that a white film is deposited on the electrode at $E > -0.4$ V SCE, and removed at $E > 0.9$ V SCE just prior to oxygen evolution. The surface remained bright for the entire negative potential sweep.

As shown in Fig. 4 the platinum sulphide/sulphur film that forms on the electrode surface has a major impact on the oxidation reaction of sulphite. It is therefore not possible to quantify the sulphite concentration in a solution by measuring the limiting current density if sulphide is present in the solution.

As can be seen in sweep 3a in Fig. 3 dithionite is oxidised to sulphite in the potential range from -0.5 to 0.4 V SCE. This potential range is lower than the oxidation potential for sulphite and it should therefore be possible to separate the two reactions. CV measurements were performed where sulphite was added stepwise to an alkaline 10 mM dithionite solution. The voltammograms are shown in Fig. 9.

Fig. 9 shows that the current peak from the oxidation of dithionite to sulphite, called peak I in the figure, disappears when the sulphite concentration is increased. This indicates that the oxidation of dithionite starts at a higher potential when sulphite is also present in the solution and that this start potential increases with increasing sulphite concentration. The reaction mechanism for the oxidation of sulphite showed that the reaction products might be strongly adsorbed to the electrode [12]. If the adsorbed products are not removed between each sweep, the oxidation of dithionite will take place on a surface covered with these products instead of a pure platinum or platinum oxide surface. The increase in the start potential for the dithionite oxidation reaction may therefore be explained by a passivation of the electrode from the reaction product of the sulphite oxidation.

The current density of the second peak in Fig. 9, called peak II, is higher than what was observed in a pure sulphite solution. This also indicates that the current density of peak II is the sum of current contributions from the oxidation of both sulphite and dithionite.

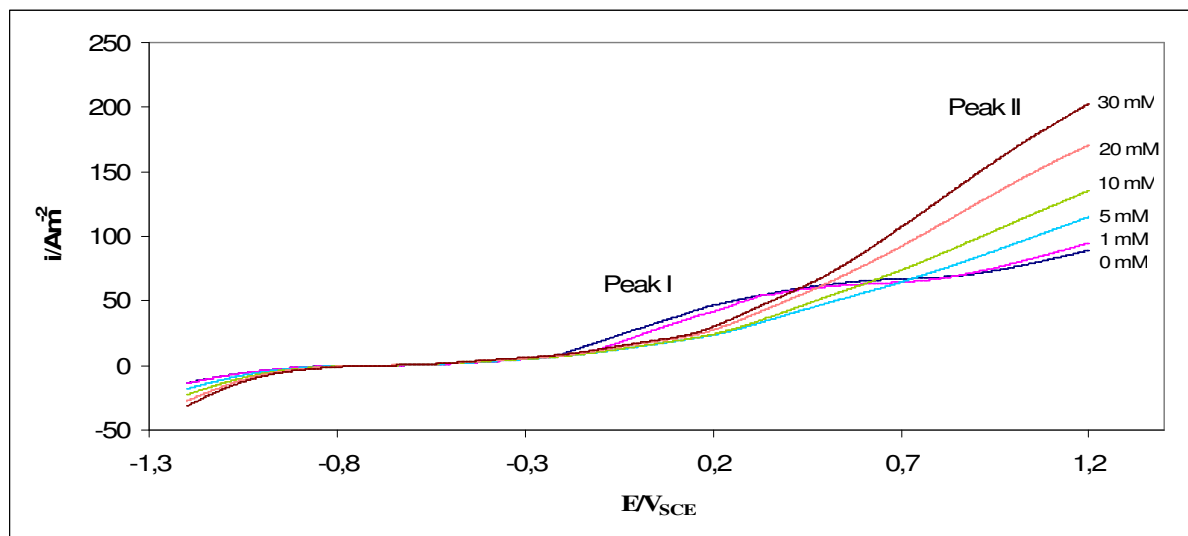


Figure 9. Voltammograms of the oxidation of stepwise added sulphite to a 10 mM dithionite on a platinum RDE. The sweep rate was 100 mV/sec, pH 11, 1000 rpm.

The observed increase in the oxidation potential of dithionite with an addition of sulphite should also be present after the first sweep with a pure dithionite solution since sulphite is produced from the oxidation of dithionite. Cyclic voltammetry experiments were therefore performed with a dithionite solution. The results are shown in Fig. 10.

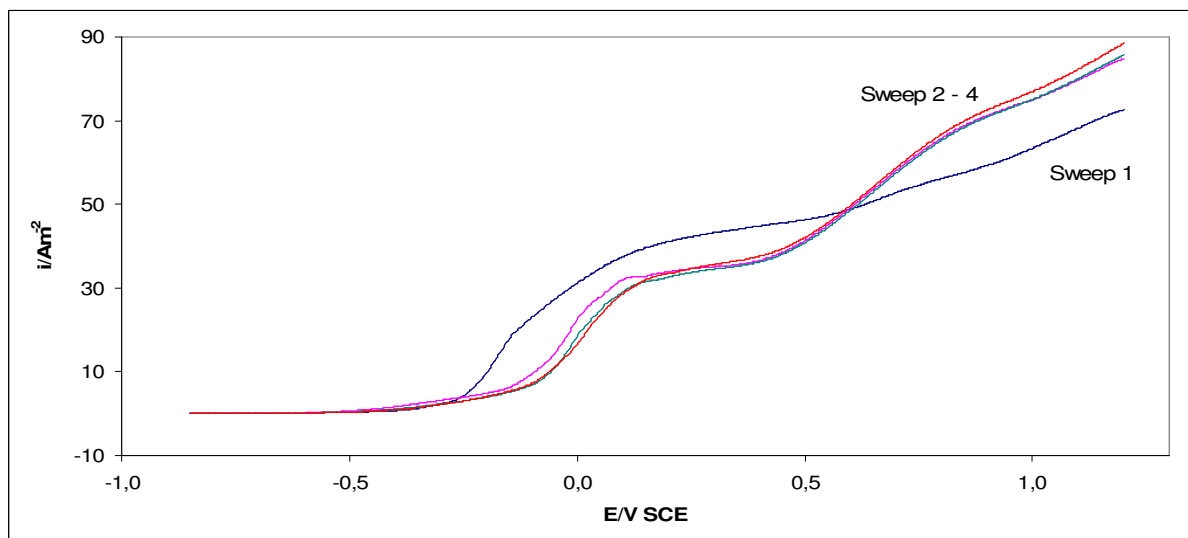


Figure 10. Voltammograms of the oxidation of 20 mM dithionite on a platinum rotating disc electrode. The sweep rate was 20 mV/sec, pH 11, 100 rpm.

Fig. 10 shows four separate sweeps. The time elapsed between the start of the first and the last of these sweeps is approximately 90 minutes. It can be seen that the start potential of the first oxidation

step of dithionite is changed to higher potentials between the first and second sweep. This is consistent with the results in Fig. 9. It can also be seen that after sulphite is formed in the first sweep, the limiting current density of the first oxidation step decreases and the current density of the second oxidation step increases in sweep 2. The remaining sweeps are independent of time.

In a pure sulphite solution the current density in a chronoamperometric experiment was found to be a linear function of the sulphite concentration raised to the power of $3/2$ [7]. This relationship is explained by the reaction mechanism of the sulphite oxidation. A strongly adsorbed sulphite radical is formed in the oxidation of sulphite. Two sulphite radicals then combine to form dithionate, which decomposes to sulphite and sulphate. The total current is therefore the sum of the oxidation of sulphite that is transported to the electrode by diffusion and the oxidation of sulphite regenerated from the oxidation product by the following chemical reactions.

In the experiments with cyclic voltammetry the exposure time at oxidative potentials is much less than in a chronoamperometric experiments, which last for approximately one hour. Thus, it is less time to achieve equilibrium in the CV experiments.

The contribution from the regenerated reactant will therefore be smaller and the current density is closer to be a linear function of the concentration of sulphite. However, when a linear regression line is fitted to the data it does not pass through origin at zero current. The intercept with the concentration axis gives a sulphite concentration of approximately 2.6 mM. This result indicates that at least some of the sulphite is still regenerated at the electrode surface. The current densities obtained at 1.05 V in Fig. 9 are plotted as a function of the sulphite concentration and as a function of the sulphite concentration raised to the power of $3/2$. For comparison the current density data from a pure sulphite solution plotted as a function of concentration is included in the figure.

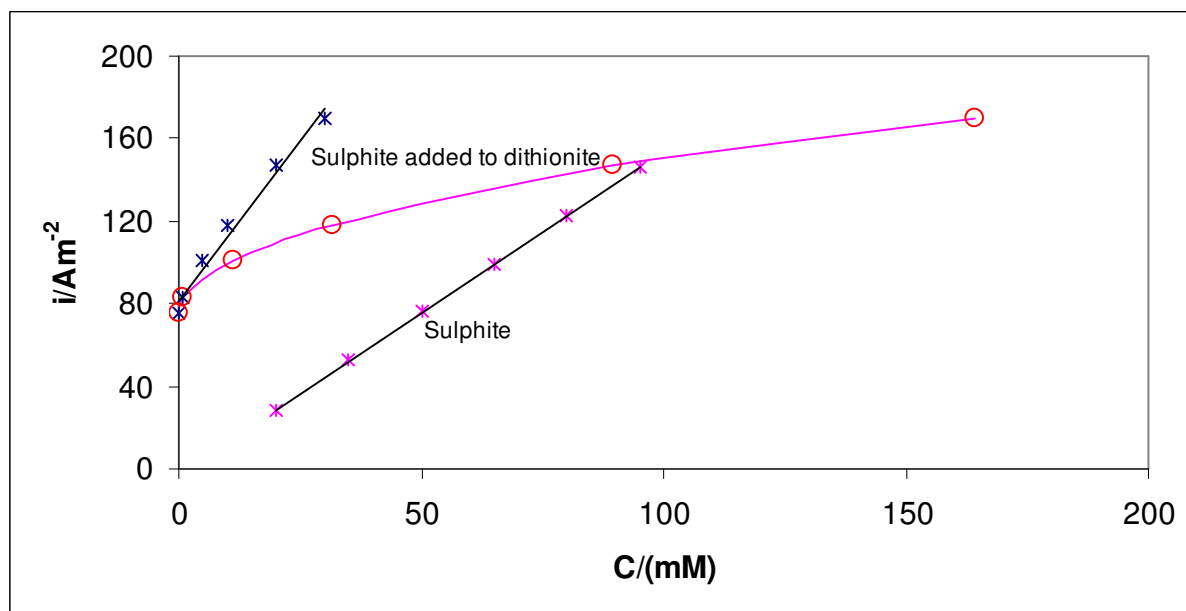


Figure 11. Current density as a function of sulphite concentration in water and 10 mM dithionite electrolyte at pH 11. Data from the mixed solution is also plotted as a function of concentration in the power of $3/2$ as open bullets (O).

As can be seen from Fig. 11 the current density in the sulphite/dithionite solution is not a exact linear function of the concentration of sulphite nor the concentration of sulphite raised to the power of $3/2$, but the relationship between the current density and the sulphite concentration gives the best fit to a linear curve. It is therefore not possible to quantify very accurate the sulphite concentration in a solution by measuring the limiting current density if dithionite is also present in the solution.

This result is not fully understood but the shift in potential for the start of the dithionite oxidation with increasing sulphite concentration might be the reason for the lack of linearity between the current density and the concentration. More work is needed to explain these observations.

4. CONCLUSIONS

- The oxidation reaction of sulphite on a platinum electrode is greatly affected when sulphide is added to the solution.
- The reaction rate of the first oxidation step of sulphide is slow.
- Analysis of the product of sulphide oxidation reaction at 1.2 V SCE shows that it consists of an outer layer of elementary sulphur and possibly a thin inner layer of platinum sulphide.
- Chronoamperometric experiments with a sulphide solution indicate that that the nucleation process is two-dimensional at 0.55 V SCE, and that the nucleation process is three-dimensional at 1.2 V SCE.
- Dithionite also affects the oxidation of sulphite. The linear relationship between the current density and the sulphite concentration raised to the power of $3/2$ could not be obtained when dithionite was present in the solution.

References

1. L. Brown, L. Szekeres, *Talanta* 26 (1979) 414.
2. W. P. Kilroy, *Talanta* 27 (1979) 343.
3. W. P. Kilroy, *Talanta* 30 (1983) 419.
4. E. P. Serjeant, *Potentiometry and Potentiometric Titrations*, Wiley, Chicester, 1984.
5. A. J. Bard, R. Parsons, J. Jordan, *Standard Potentials in Aqueous Solution*, Marcel Decker, New York, 1985.
6. E. Gasana, P. Westbroek, K. De Wael, E. Temmerman, K. De Clerck, P. Kiekens, *J. Electroanal. Chem.* 553 (2003) 35.
7. E. Skavås, A. Adriaens, T. Hemmingsen, *Int. J. Electrochem. Sci.* 1 (2006) 414.
8. A. Einarsson, E. Gunnlaugsson, *Proceedings of Cold Climate HVAC* (1997) 161.
9. N. Ramasubramanian, *J. Electroanal. Chem.*, 64 (1975), 21.
10. E. Gasana, P. Westbroek, E. Temmerman, H. P. Thun, P. Kiekens, *Anal. Chim. Acta* 486 (2003) 73.
11. E. Gasana, P. Westbroek, E. Temmerman, H. P. Thun, *Anal. Commun.* 36 (1999) 387.
12. E. Skavås, T. Hemmingsen, *Electrochim. Acta*, In press.
13. A. Q. Contractor, H. Lal, *J. Electroanal. Chem.* 93 (1978) 99.
14. D. Pletcher, R. Greef, R. Peat, L.M. Peter, and J. Robinson, *Instrumental Methods in Electrochemistry* (Herwood Publishing Ltd, 2001).
15. M. G. Dowsett, *Appl. Surface Sci.*, 203-204 (2003) 5.

16. H. R. Thirsk, J. A. Harrison, A guide to the study of electrode kinetics, Academic Press, London, 1972, Chapter 3.
17. M. Palomar-Pardavé, M. T. Ramirez, I. González, A. Serruya, B. Sharifker, *J. Electrochem. Soc.*, 143 (1996) 1539.
18. M. Palomar-Pardavé, M. Margarita-Hernández, I. González, N. Batina, *Surface Science*, 399 (1998) 80.
19. S. Kapusta, A. Viehbeck, S. M. Wilhelm, N. Hackerman, *J. Electroanal. Chem.* 153 (1983) 157.

© 2007 by ESG (www.electrochemsci.org)
